VNS23(5) 23008 1/8 06/29/06 13:38 pm

log no. VNS 23008

Visual Neuroscience (2006), **23**, 1–8. Printed in the USA.

DOI: 10.1017/S0952523806230086

When S-cones contribute to chromatic global motion processing

ALEXA I. RUPPERTSBERG, SOPHIE M. WUERGER, AND MARCO BERTAMINI

Department of Psychology, University of Liverpool, Eleanor Rathbone Building, Liverpool, United Kingdom

(RECEIVED July 6, 2005; ACCEPTED April 25, 2006)

Abstract

There is common consensus now that color-defined motion can be perceived by the human visual system. For global motion integration tasks based on isoluminant random dot kinematograms conflicting evidence exists, whether observers can (Ruppertsberg et al., 2003) or cannot (Bilodeau & Faubert, 1999) extract a common motion direction for stimuli modulated along the isoluminant red-green axis. Here we report conditions, in which S-cones contribute to chromatic global motion processing. When the display included extra-foveal regions, the individual elements were large (~0.3°) and the displacement was large (~1°), stimuli modulated along the yellowish-violet axis proved to be effective in a global motion task. The color contrast thresholds for detection for both color axes were well below the contrasts required for global motion integration, and therefore the discrimination-to-detection ratio was >1. We conclude that there is significant S-cone input to chromatic global motion processing and the extraction of global motion is not mediated by the same mechanism as simple detection. Whether the koniocellular or the magnocellular pathway is involved in transmitting S-cone signals is a topic of current debate (Chatterjee & Callaway, 2002).

Keywords: Color, Motion, S-cones, Random dot kinematogram, Isoluminance

Introduction

There is consensus now that purely chromatic motion mechanisms exist, which are different from the luminance motion mechanism (Cavanagh et al., 1985; Cropper & Derrington, 1996; Derrington & Badcock, 1985; Dougherty et al., 1999; Mullen & Baker, 1985; Ruppertsberg et al., 2003; Seidemann et al., 1999; Wandell et al., 1999); for a recent review see (Cropper & Wuerger, 2005). The main argument for the difference between these mechanisms is that the motion discrimination-to-detection threshold ratio for luminance-defined motion stimuli is close to one (Levinson, 1975; Watson et al., 1980) indicative of a single mechanism that detects the presence of the stimulus and extracts its motion. For chromatic (isoluminant red-green) stimuli, however, this ratio is significantly higher (Cavanagh & Anstis, 1991; Derrington & Henning, 1993; Kooi & DeValois, 1992; Lindsey & Teller, 1990; Metha & Mullen, 1998; Metha et al., 1994; Mullen & Boulton, 1992; Palmer, Mobley et al., 1993), which is usually taken as evidence that different mechanisms mediate the detection and the motion extraction in isoluminant chromatic stimuli. The discrimination-to-detection ratio is influenced by stimulus duration with shorter durations requiring higher contrasts for motion discrimination than for detection (Cropper & Derrington, 1994, 1996). The ratio is further influenced by eccentricity. Detection thresholds increase more rapidly for chromatic than for achromatic stimuli with increasing eccentricity (Metha et al., 1994; Mullen, 1985, 1991) and color contrast thresholds for direction discrimination show a dramatic fall-off with eccentricity in comparison to detection performance (Bilodeau, 1997).

Virtually all studies discussed early investigated the input of the putative red-green mechanism to motion processing; this mechanism is assumed to be cone-opponent taking the difference between the L- and M-cones. Here we attempt to characterize the role of the S-cones in global motion processing by using chromatic modulations that isolate the putative yellowish-violet mechanism (S–(L + M)) (Derrington et al., 1984). We used random dot kinematograms (RDKs) (Braddick, 1980; Newsome & Pare, 1988; Ramachandran & Gregory, 1978), in which the observer is presented with a display of moving dots. Some of the dots in the display move in the same direction ("signal dots"), whereas the rest moves in different directions ("noise dots"). The percentage of signal dots is called the coherence level of an RDK. The observer can find the direction of global motion in the display by integrating local motion vectors and extracting the prevailing motion direction. The main focus of previous chromatic global motion studies was on the interaction between the luminance and the chromatic motion signals and the role of chromatic information in image segmentation before local motion signals are combined (Britten, 1999; Croner & Albright, 1997; Edwards & Badcock, 1996; Li & Kingdom, 2001; Moeller & Hurlbert, 1997; Moeller & Hurlbert, 1997; Ramachandran, 1987; Ramachandran & Gregory, 1978; Snowden & Edmunds, 1999). Studies that focused purely on the chromatic input to global motion processing provide conflicting evidence. One study concluded that there is no or very little

Address correspondence and reprint requests to: Alexa I. Ruppertsberg, Department of Optometry, University of Bradford, Bradford, BD7 1DP, United Kingdom. E-mail: a.i.ruppertsberg@bradford.ac.uk

red-green input into global motion processing (Bilodeau & Faubert, 1999), whereas another study found a significant red-green input (Ruppertsberg et al., 2003) but no yellowish-violet input.

In this study we examined the influence of two experimental parameters on S-cone behavior and demonstrate that S-cones can mediate chromatic global motion extraction under appropriate conditions. We presented isoluminant stimuli for a range of color directions and varied blob displacement and blob size. We also measured detection thresholds to address the question whether motion discrimination is mediated by the same mechanism as simple detection. Finally, we show that the parameters under which S-cones can contribute to global motion are compatible with the anatomical differences between the cone classes.

Materials and methods

Methods and stimuli are described later but further details are in Ruppertsberg et al. (2003).

Apparatus

Experiments were run on a standard PC with a VSG2/5 graphics card (32-MB memory, Cambridge Research Systems, Ltd.). Stimulus presentation was controlled with Matlab (Mathworks) and stimuli were presented on a 21-inch CRT-monitor (SONY GDM-F500), which was calibrated using a spectroradiometer (Photo Research PR650). Observers' responses were collected using a button box (CT3, Cambridge Research Systems, Ltd.).

Participants

Five participants (three naives and two authors) took part in the study and had normal or corrected-to-normal vision. Their color vision was assessed with the Cambridge Color Test (Regan et al., 1994). Participants were paid and informed about the objective of the study and gave their signed consent.

Stimuli

We used sparse RDKs with 150 colored Gaussian blobs and a coherence level of 40%. In all experiments color contrast was varied in response to observers' responses. The RDK was presented on a grey background with a luminance value of 50 cd/m^2 and chromaticity values of $x = 0.292$ and $y = 0.306$ (CIE 1931). For each interval a new RDK was generated and all blobs moved along individual trajectories and did not have a limited lifetime. To eliminate the effect of any luminance artefacts, dynamic (two-dimensional) luminance noise was superimposed onto the RDKs; we quantified noise amplitude as root mean squared (rms) contrast and the individual values were determined experimentally and found effective to mask luminance-defined motion for our particular stimulus configurations (for determination of effective masking see (Ruppertsberg et al., 2003)).

We manipulated two parameters: blob size and blob displacement with two experimental conditions each. For blob size we had the FAR and CLOSE condition; in the FAR condition participants were seated 200 cm away from the monitor, the RDK array size was 5.1° × 4°, a single Gaussian blob had a standard deviation of 0.07° of visual angle and mean center-to-center blob separation was 0.4° of visual angle. The rms contrast of the luminance noise was 19.5%. In the CLOSE condition participants were seated 50 cm away from the monitor, the RDK array size was 19.6° × 15.6°, a single Gaussian blob had a standard deviation of 0.29° of visual angle and mean centre-to-centre blob separation was 1.5° of visual angle. The rms contrast of the luminance noise was 24%. The most likely reason for the difference in required rms contrast of the luminance noise is that the retinal size of the motion stimuli was different (for details see Ruppertsberg et al., 2003).

For blob displacement we had the SMALL and LARGE condition; in the SMALL condition blobs were displaced by 0.23° and in the LARGE condition by 1.17°.

Procedure

Before each experiment we determined each observer's point of isoluminance by heterochromatic flicker photometry (HCFP) (Walsh, 1958) and adjusted the display. For HCFP we used stimuli as similar as possible to the temporal and spatial layout of our global motion task, that is, we used the RDK stimuli (a screen with 150 Gaussian blobs and same display settings as described in Stimuli) and altered the color between red and green at 20 Hz. Participants were asked to change the luminance settings of red and green to minimize flicker. Each observer repeated this selection five times reliably and the average was taken.

In both, the motion discrimination and the detection experiment, we used a two-interval forced-choice (2IFC) paradigm. Each interval was presented for 233 ms to minimize eye movements and was preceded by a fixation period of 500 ms. After the second interval participants responded by pressing a button. They were instructed to give a correct answer, not a fast answer and were provided with acoustic feedback. The response guided a QUEST procedure (Watson & Pelli, 1983) and the estimated threshold corresponded to a performance of 81% correct responses. Each threshold was measured at least twice for each of the five participants.

In the motion discrimination experiment (Experiment 1) one interval contained leftward or rightward coherent motion and the other interval contained no coherent motion (random motion). The observer's task was to decide whether the first or the second interval contained coherent motion irrespective of its direction.

In the detection experiment (Experiment 2) one interval contained an RDK with random motion, whereas the other interval contained the grey background only (both intervals had dynamic luminance noise). Participants had to indicate, in which interval the RDK was present because color contrast was changed according to a QUEST procedure (Watson & Pelli, 1983).

Color space

To establish the color contrast thresholds for the global motion task (Experiment 1) and the detection task (Experiment 2) we used the DKL-color space (Brainard, 1996; Derrington et al., 1984). We characterize the chromatic properties of our stimuli by the responses of the underlying mechanisms rather than by the cone coordinates of the stimuli that isolate these mechanisms. The three corresponding mechanisms are two cone-opponent color mechanisms and a luminance mechanism. One cone-opponent color mechanism is the red-green mechanism that takes the weighted difference between the differential M- and the L-cone excitations and the other cone-opponent color mechanism is the yellowish-violet mechanism that takes the weighted difference between the differential S-cone and the summed differential M- and L-cone excitations. The luminance mechanism sums the weighted differential M- and L-cone signals. For the sake of simplicity, the two

color mechanisms are referred to as M–L and S–(L+M) mechanisms (Derrington et al., 1984) or as "red-green" and "yellowish-violet" mechanisms, because this reflects the color appearance of the modulations when seen on a neutral background (Cropper & Wuerger, 2005).

Our figures show the isoluminant plane of the two color mechanisms and polar coordinates are used to refer to a point in this plane (angle φ, radius r). Hue changes with the angle and contrast changes with the radius (which is loosely related to saturation). The central point (0, 0) corresponds to the grey background and its cone coordinates were: L = 32.42, M = 17.58, S = 1.055. The endpoints of the M–L axis are green ("G," polar coordinates: (0, 1), cone coordinates L = 30.39, M = 19.61, S = 1.05), and red ('R', polar coordinates: (180, 1), cone coordinates L = 34.45, M = 15.55, S = 1.05). The endpoints of the S–(L + M) axis are violet ("V" polar coordinates: (90, 1), cone coordinates L = 32.42, M = 17.58, S = 1.8) and yellowish ("Y" polar coordinates: (270, 1), cone coordinates L = 32.42, M = 17.58, S = 0.31). A radius of 1 along the M-L axis corresponds to about 6% modulation in the L cones and 11% modulation in the M cones; along the S(L + M) axis a radius of 1 corresponds to an S-cone contrast of about 70%.

Experiment 1—motion discrimination thresholds for different blob sizes and displacements

We determined color contrast thresholds for global motion integration in the isoluminant color plane (S–(L + M) *vs*. M–L) for eight different color directions (0°, 45°, 90°, 135°, 180°, 225°, 270°, and 315°). Observers had to distinguish between an RDK with random motion and an RDK with 40% coherent motion (2IFC). All blobs had the same color contrast in a given trial and were presented on a grey background (see Materials and methods). Two parameters were manipulated: blob displacement and blob size. Blob displacement was either SMALL (0.23°) or LARGE (1.17°). Blob size was manipulated by varying viewing distance; for the FAR condition (viewing distance 200 cm) the individual blobs in the RDK were 0.07° and in the CLOSE condition (viewing distance 50 cm) 0.29°. The RDK array size changed accordingly from 5.1° × 4° to 19.6° × 15.6°. Had we changed the blob size while keeping the RDK array size constant at 5.1° × 4°, the number of Gaussian blobs in an RDK would have reduced to less than 30 blobs. Each of the four permutations was tested separately (Table 1) in random order for each of the three observers (one author and two naïve participants). Data represent the mean of two threshold measurements.

Table 1. *Conditions and parameter values in Experiment 1. The first number in each pair refers to the blob size and the second number (italics) to the displacement. The rms contrast of the dynamic luminance noise overlaid onto the stimuli was 19.5% for the FAR and 24% for the CLOSE condition (see Materials and methods)*

	Blob displacement	
Blob Size	Small	Large
Far	0.07°/*0.23°*	0.07°/*1.17°*
Close	0.29°/*0.23°*	0.29°/*1.17°*

Results

In Fig. 1 the color contrast thresholds for global motion integration are plotted. Each data point is defined by an angle and its distance from the origin (which corresponds to the background). The red-green axis is labeled "G" (0°) and "R" (180°) and the yellowish-violet axis "V" (90°) and "Y" (270°). Each experimental condition is represented by symbols over the columns. From left to right they are: small blobs and small displacement (FAR/SMALL condition), small blobs and large displacement (FAR/LARGE), large blobs and small displacement (CLOSE/SMALL) and large blobs and large displacements (CLOSE/LARGE).

In the FAR/SMALL condition all observers were able to use the chromatic signal along the red-green axis to extract motion. Their thresholds (expressed as radius) varied from 0.75 for observer CH to 0.98 for observer JM. For all observers, the thresholds were roughly symmetric around the white point indicating that increments and decrements in both L- and the M-cones were equally effective. However, along the yellowish-violet axis (270° and 90°) participants were not able to respond reliably and no threshold could be determined. Participants stated independently that the stimuli were clearly visible but they were not able to see any coherent movement for isoluminant yellowish or violet colors.

Similar results were obtained when the displacement was increased (FAR/LARGE); chromatic signals along the red-green axis could be used to extract motion, but not along the yellowish-violet axis. Thresholds along the red-green axis varied from 0.73 for observer CH to 1.1 for observer AR. As in the FAR/SMALL condition, thresholds were roughly symmetric around the white point.

When the blobs were four times larger but displacement was small (CLOSE/SMALL) all thresholds increased, but again, chromatic signals along the yellowish-violet axis could not be used to extract motion. Thresholds varied from 0.96 for observer AR to 1.22 for observer JM and were roughly symmetric around the white point.

When blob size and displacement were large (CLOSE/LARGE) global motion integration was possible for chromatic signals modulated not only along the red-green but also along the yellowish-violet axis. The thresholds along the red-green axis varied from 0.74 for observer JM to 1.22 for observer JM (JM had the lowest and highest value) and along the yellow-blue axis from 0.74 for observer CH to 0.97 for observer CH (CH had the lowest and highest value). The thresholds were not as symmetric around the white point as in the previous conditions. We found lower thresholds for S-cone decrements (270° condition: 0.78, 0.74, 0.90 for observers AR, CH, and JM) than for S-cone increments (90° condition: 0.92, 0.97, 0.95 for observers AR, CH, and JM) and a similar asymmetry along the red-green axis with lower thresholds for M-cone increments and L-cone decrements (180° condition: 0.76, 0.75, 0.75 for observers AR, CH, and JM) than for M-cone decrements and L-cone increments (0° condition: 0.81, 1.03, 1.22 for observers AR, CH, and JM).

In summary, only when large displacements (~1°) were combined with large blobs (~0.3°) S-cone modulations could be used to extract global motion.

Experiment 2—detection thresholds

Having identified parameters for global motion integration for stimuli modulated along the red-green and the yellowish-violet axis we can address the question whether different mechanisms

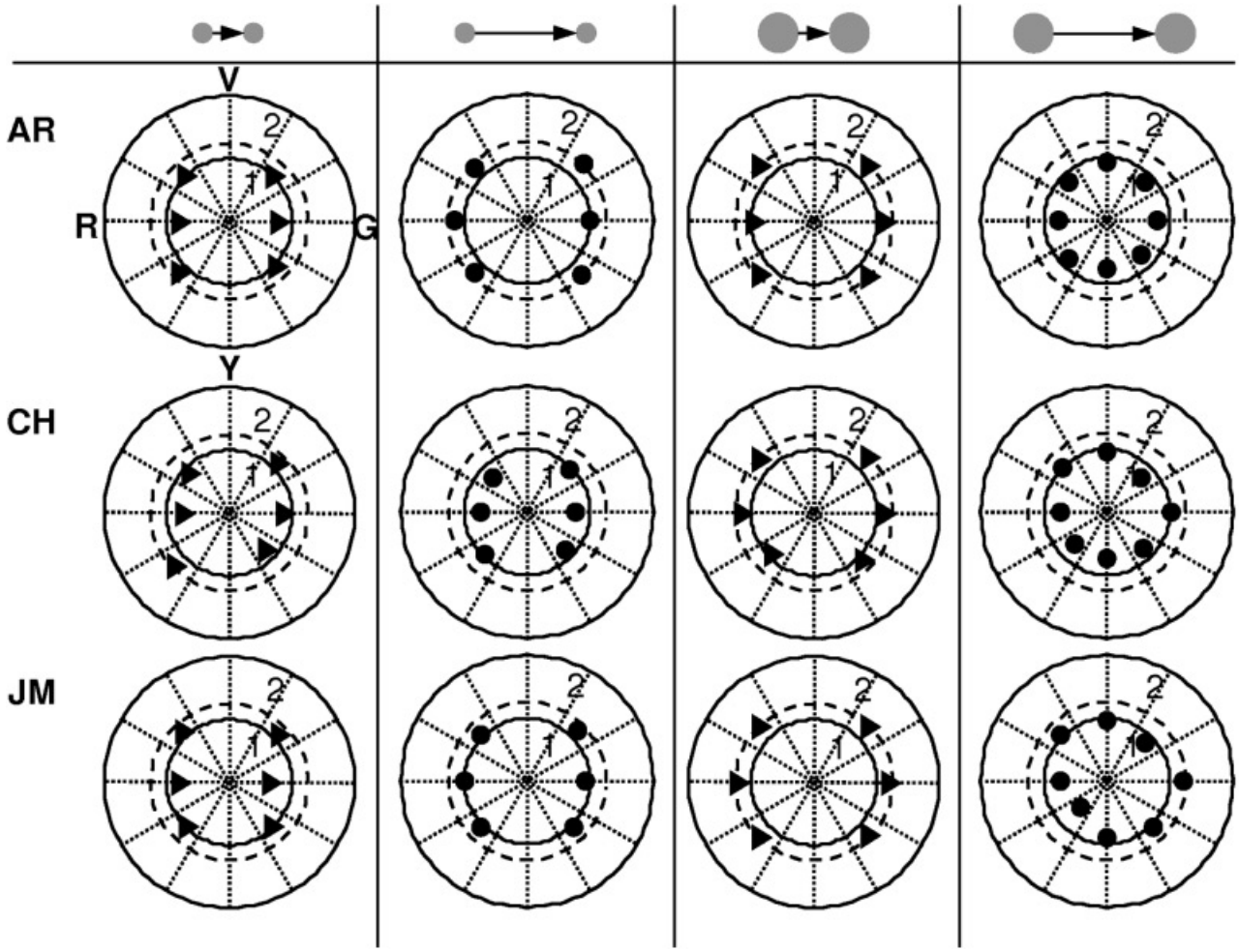

Fig. 1. Discrimination thresholds in Experiment 1 for three observers (rows) and four different stimulus conditions (columns). From left to right: FAR/SMALL condition, dot size 0.07 deg and dot displacement 0.23 deg; FAR/LARGE condition, dot size 0.07 deg and dot displacement 1.16 deg; CLOSE/SMALL condition, dot size 0.29 deg and dot displacement 0.23 deg; CLOSE/LARGE condition, dot size 0.29 deg and dot displacement 1.16 deg. All plots share the axis labelling of the top left. The inner solid circle corresponds to a radius r = 1, the outer solid circle to r = 2.

mediate the detection and motion extraction for modulations in the isoluminant plane. To compute the discrimination-to-detection ratio for global motion we measured color contrast detection thresholds in the cone-opponent color space (S–(L + M) *vs*. M–L) for the same eight color directions as in Experiment 1. Blob size and displacement were large (CLOSE/LARGE) because this was the only condition where S-cone modulations could be used for global motion extraction. The same three observers from Experiment 1 and two additional observers participated in Experiment 2 (one author (MB) and one naïve observer (EP)). Their motion discrimination thresholds for the CLOSE/LARGE condition were also measured and are presented in Fig. 2b. Data represent the mean of three threshold measurements.

Results

Detection thresholds in polar coordinates for all observers are plotted in Fig. 2a. For all color directions in the isoluminant plane, participants were able to detect the stimuli at much lower color contrasts than required for the global motion task. Note that the scale of the discrimination threshold (Fig. 1 and Fig. 2b) plots is twice as large as for the detection threshold data (Fig. 2a). The mean contrast detection threshold across all observers was 0.19 (expressed as radius), whereas the mean motion discrimination threshold was 0.88 for the CLOSE/LARGE condition.

In Fig. 3a the motion discrimination and detection thresholds are plotted in Cartesian coordinates, namely radius (threshold) as a function of color angle. The contrast thresholds (in terms of radius) for motion discrimination vary from about 0.7–1.2; for detection they range from 0.1 to 0.4. In Fig. 3b, the motion discrimination-to-detection threshold ratio is plotted as a function of the color angle in the isoluminant plane. First and foremost we find that the global motion threshold to detection threshold ratio was always >1, ranging between 3 and 8. Therefore, different mechanisms must mediate global motion processing and detection of the chromatic stimuli in the isoluminant plane. Second, the threshold ratio stayed constant (in the range of 3–5) across all color angles for three out of five observers (AR, CH, and EP; open symbols). The ratios of the other two observers (JM and MB; filled symbols) reached a minimum with comparable values to the three

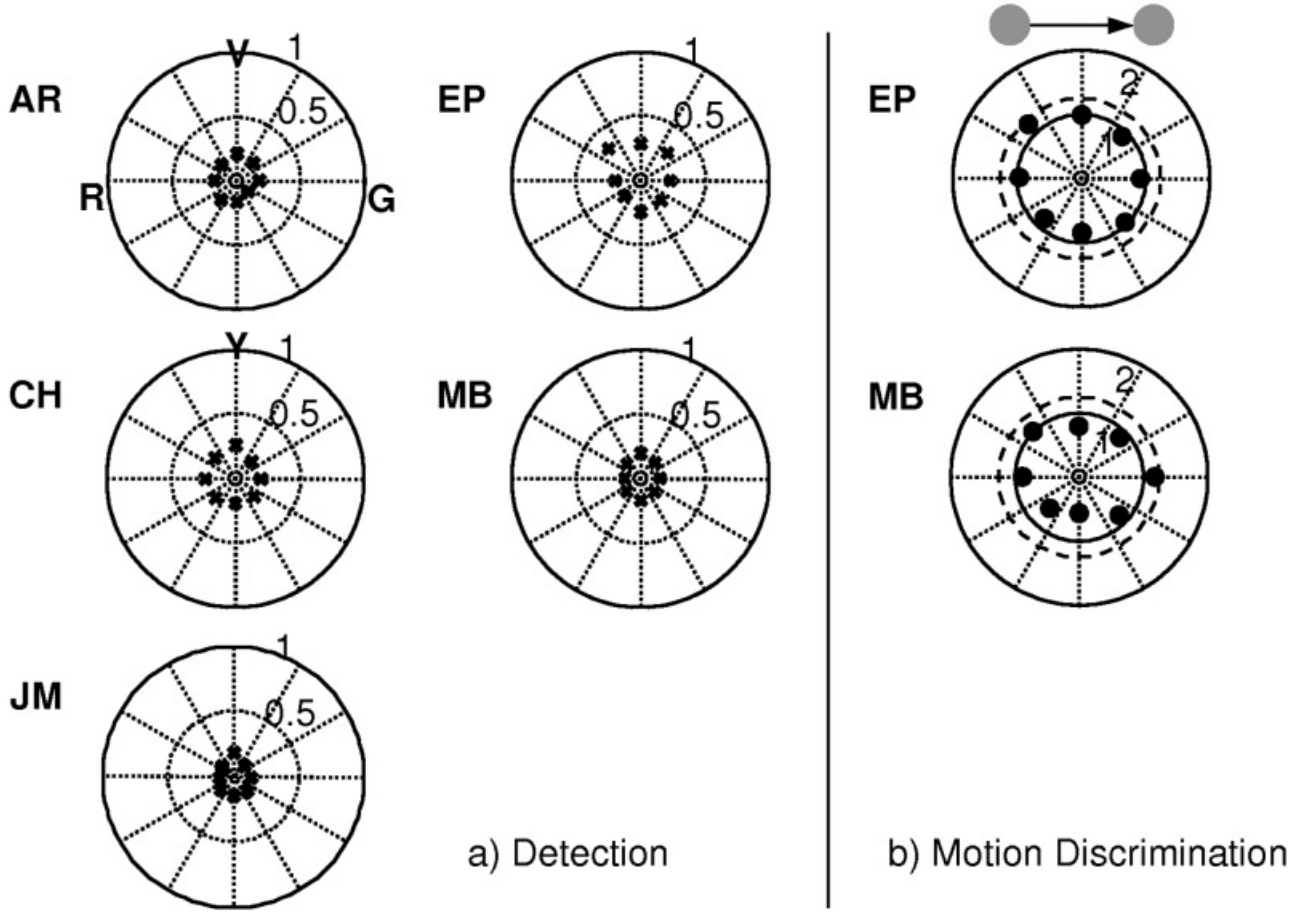

Fig. 2. (a) Detection thresholds in Experiment 2 in the CLOSE/LARGE condition (dot size 0.29°, dot displacement 1.16°). Left column: same three observers as in Experiment 1. Middle column: two additional observers. (b) Discrimination thresholds in the CLOSE/LARGE condition (dot size 0.29°, dot displacement 1.16°) for the two additional observers. All plots share the axis labeling of the top left. The inner circle corresponds to a radius r = 0.5, the outer circle to r = 1.

observers (around 5) at about 90° and 270°, which corresponds to the yellowish-violet axis. For the other color angles it was larger (up to 8.5 for 0 and 135° for JM and up to 7.6 for 0 and 180° for MB). The cause for the variability in ratios stemmed from the motion discrimination thresholds because the detection thresholds did not vary substantially (Fig. 3a; standard deviation of detection thresholds: AR: 0.021, CH: 0.025, JM: 0.026, EP: 0.058, and MB: 0.021). The two observers with varying ratio values (JM and MB) had the largest standard deviations for their discrimination thresholds (AR: 0.062, CH: 0.131, JM: 0.19, EP: 0.113, and MB: 0.189).

Discussion

It has been shown that human observers can perceive motion from purely chromatic motion stimuli (Cavanagh et al., 1985; Cropper & Derrington, 1996; Derrington & Badcock, 1985; Dougherty et al., 1999; Mullen & Baker, 1985; Seidemann et al., 1999; Wandell et al., 1999), including from global motion stimuli like RDKs (Ruppertsberg et al., 2003) and plaid stimuli (Cropper et al., 1996; Krauskopf & Farell, 1990). Chromatic motion mechanisms are different from the luminance motion mechanism because the motion discrimination-to-detection threshold ratio for isoluminant red-green stimuli is significantly higher than 1 (Cavanagh & Anstis, 1991; Derrington & Henning, 1993; Kooi & DeValois, 1992; Lindsey & Teller, 1990; Metha & Mullen, 1998; Metha et al., 1994; Mullen & Boulton, 1992; Palmer et al., 1993), indicating that different mechanisms mediate the detection and the motion extraction in isoluminant chromatic stimuli.

In this study we investigated the red-green (L-M) and the S-cone input to global motion perception. Whereas in a previous study S-cone modulations were found to be ineffective for global motion extraction (Ruppertsberg et al., 2003), we demonstrated here that global motion can be extracted from an RDK defined solely by S-cone modulations provided that the blobs (∼0.3°) and displacement were large (∼1°). This S-cone input to global motion was genuine and could not be explained by potential luminance artefacts. Similarly to isoluminant red-green motion targets our results are consistent with the idea that different mechanisms mediate global motion extraction and simple detection of S-cone isolating targets, because the motion discrimination-to-detection threshold ratio was >1. Our findings corroborate conclusions drawn by Stromeyer et al. (1995) who found that along a red-green (however, not necessarily isoluminant) axis two mechanisms operate at threshold, one tuned to detect the presence and the hue of a stimulus, the other tuned to discriminate its motion. Our experiments further extend these results by showing that different

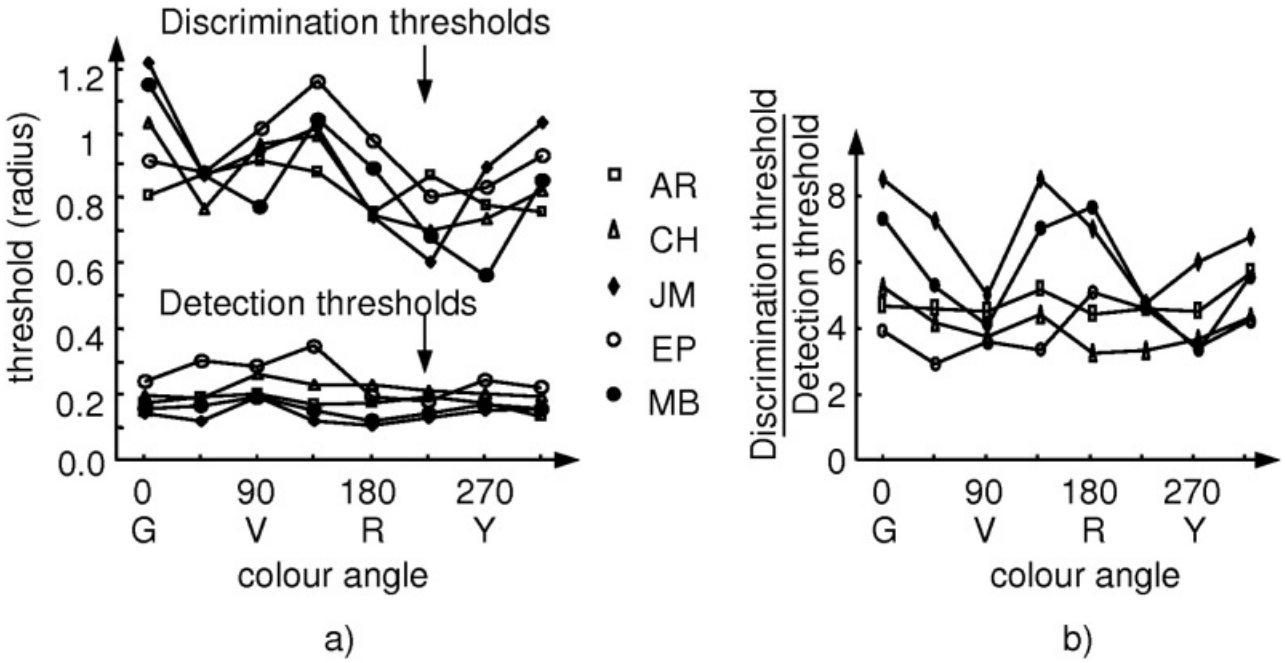

Fig. 3. (a) Discrimination and detection thresholds from Experiments 1 and 2 over different color angles for all observers and mean ("m"). (b) Discrimination threshold to detection threshold ratios over different color angles for all observers and mean ("m"). Bars indicate +/− 1 STD. "G" = green, "V" = violet, "R" = red, "Y" = yellowish.

detection and motion mechanisms must also be at work for S-cone modulated targets.

Parameters for S-cone contribution to chromatic global motion processing

Whether S-cones contribute to motion perception has attracted considerable interest in the last years. Whereas the idea of a completely "color-blind" motion system has been largely discredited and there is now compelling evidence for a red-green (L-M) input to motion perception (for a recent review see (Cropper & Wuerger, 2005)), the evidence on the magnitude and the nature of the S-cone input to the motion system is still conflicting (Sincich & Horton, 2005). One possibility is that S-cones contribute to motion perception by feeding into the magnocellular pathway (Calkins, 2001; Chatterjee & Callaway, 2002). An alternative explanation is that there is a direct input from the koniocellular LGN layers (which are driven by S-cones) to motion-sensitive striate and extrastriate areas (Hendry & Reid, 2000; Sincich et al., 2004). Recent neurophysiological evidence is consistent with the former hypothesis; the strength of the observed S-cone input to MT relative to the L and M cone input is consistent with its relative input to the magnocellular layers of LGN and their relative occurrence in the retina (Barberini et al., 2005). The available behavioral evidence for an S-cone input to motion is not always consistent and part of the discrepancy may be because of the differences in stimulus configuration. In our experiment we varied two relevant parameters, namely the size of the local motion signals and the displacement, and we identified spatial configurations under which S-cones provide an effective input to global motion processing.

In Experiment 1 we varied the blob size and blob displacement in our RDKs. We could not find S-cone contribution when the blobs were small and moved only a short distance (FAR/SMALL condition) or when they moved a farther distance within the same time window (FAR/LARGE). The display area for these conditions was 5.1° × 4° and thus covered the entire fovea. There is an S-cone free area in the center of the fovea of about 0.3° to 0.4° (Bumsted & Hendrickson, 1999), but the density for S-cones peaks just outside of the central fovea at about 1° to 2° (Curcio et al., 1991). It is therefore unlikely that the limiting factor for the S-cone input to motion is a lack of spatial resolution due to the S-cone spacing in the retina (10 arc min; (Wandell, 1993)). The stimuli can be easily resolved in each individual frame (peak energy—apart from the DC component—at 2.9 cpd for the FAR condition, and at 0.75 cpd for the CLOSE condition, which is well within the spatial acuity provided by the S-cones). Given an S-cone spacing of 10 arc min and the displacement by either 0.23° or 1.17°, each individual blob is seen by an average of 1.4 or 7 S-cones. There is also little convergence in the fovea and a single S-cone provides the dominant input (70%) to a particular ganglion cell (Calkins, 2001; Chichilnisky & Baylor, 1999). This suggests that the lack of S-cone input to global motion when the individual motion elements are small is due to post-retinal limitations of the S-cone pathway and not to spatial summation within the retina.

When the displacement (1.17°) and the individual elements (0.29°) were large (CLOSE/LARGE condition) we found a significant S-cones contribution to global motion processing. Because the increase in blob size was achieved by reducing the viewing distance to the display, the display area increased from 5.1 × 4° to 19.6 × 15.6°, including now large areas of extra-foveal retina. From about 4° eccentricity the fraction of S-cones stays constant at about 7% (Curcio et al., 1991). Since S-cones are fairly low in numbers in the cone mosaic in contrast to M- and L-cones and are distributed in a quasi-regular fashion over most of the retina (Calkins, 2001) increasing the display area will contribute to a stronger S-cone signal. Psychophysical evidence of differential

distributions of red-green and yellow-blue cone opponency across the visual field confirms this notion (Mullen & Kingdom, 2002). The retinal ganglion cell associated with S-cones is the small bistratified ganglion cell (Dacey & Lee, 1994). In the macaque fovea typically three S-cones connect to two to three bipolar cells, which in turn feed into one small bistratified ganglion cell; at 10°–20° eccentricity one small bistratified ganglion cell collects signals from 5 to 10 S-cones (Calkins, et al., 1998; Chichilnisky & Baylor, 1999). This pooling may be the reason why enlarging the blobs was a significant stimulus manipulation, but why the displacement had to be sufficiently large to detect motion.

Detection and chromatic global motion thresholds and ratios

In Experiment 2 we measured detection thresholds for our stimuli in the CLOSE/LARGE condition. Detection thresholds were very low in comparison to global motion thresholds and symmetrical along the tested axes. These detection thresholds were similar to the detection thresholds we had obtained for the FAR/SMALL condition (Ruppertsberg et al., 2003). Because detection thresholds increase with increasing eccentricity (Metha et al., 1994; Mullen, 1985, 1991), we may have expected an increase in detection thresholds in the CLOSE/LARGE condition because large extra-foveal areas were stimulated. Because the foveal area continued to be stimulated and because the concurrent manipulation of display and blob size presumably did not affect the amount of colored area falling onto the fovea we did not find a change in detection thresholds.

The values of the motion discrimination-to-detection threshold ratio ranged between 3 and 8 indicating that different mechanisms mediate the chromatic global motion extraction and the detection of S-cone defined targets. Furthermore, this ratio was constant for all measured color directions for three out of five observers. The other two observers had increased, but not significantly different ratios for all but the yellowish-violet axis, which was because of the variability in the discrimination thresholds (Fig. 3a). All ratio values were similar to those previously found for red-green modulated targets (Ruppertsberg et al., 2003).

In conclusion, our results suggest that S-cone modulations can mediate chromatic global motion processing under appropriate stimulus conditions. However, this motion-sensitive mechanism is different from the mechanism that detects the presence of the chromatic target. It has been shown that cortical motion areas receive S-cone input (Barberini et al., 2005; Dougherty et al., 1999; Morand et al., 2000; Seidemann et al., 1999; Wandell et al., 1999). Whether isoluminant S-cone targets are likely to stimulate the koniocellular pathway (DeValois et al., 2000), the parvocellular (Derrington et al., 1984; Stromeyer et al., 1998), or magnocellular pathway (Chatterjee & Callaway, 2002) is a topic of current debate.

Acknowledgments

The authors thank Jasna Martinovic for her assistance in running the experiments. This project was funded by the Wellcome Trust No. 058513 (to S.M.W. and M.B.).

References

Barberini, C.L., Cohen, M.R., Wandell, B. & Newsome, W.T. (2005). Cone signal interactions in direction-selective neurons in the middle temporal visual area (MT). *Journal of Vision* **5**, 603–621.

Bilodeau, L. & Faubert, J. (1999). Global motion cues and the chromatic motion system. *Journal of the Optical Society of America A* **16**, 1–5.

Bilodeau, L. & Faubert, J. (1997). Isoluminance and chromatic motion perception throughout the visual field. *Vision Research* **37**, 2073–2081.

Braddick, O.J. (1980). Low-level and high-level processes in apparent motion. *Philosophical Transactions of the Royal Society London B* **290**, 137–151.

Brainard, D. (1996). Cone contrast and opponent modulation color spaces. In *Human Color Vision*, eds., Kaiser & Boynton, pp. 563–579. Washington, DC: Optical Society of America.

Britten, K.H. (1999). Motion perception: How are moving images segmented? *Current Biology* **9**, R728-R730.

Bumsted, K. & Hendrickson, A. (1999). Distribution and development of short-wavelength cones differ between *Macaca* monkey and human fovea. *Journal of Comparative Neurology* **403**, 502–516.

Calkins, D.J. (2001). Seeing with S cones. *Progress in Retinal and Eye Research* **3**, 255–287.

Calkins, D.J., Tsukamoto, Y. & Sterling, P. (1998). Microcircuitry and mosaic of a blue/yellow ganglion cell in the primate retina. *Journal of Neuroscience* **18**, 3373–3385.

Cavanagh, P. & Anstis, S. (1991). The contribution of color to motion in normal and color-deficient observers. *Vision Research* **31**, 2109–2148.

Cavanagh, P., Boeglin, J. & Favreau, O.E. (1985). Perception of motion in equiluminous kinematograms. *Perception (OZD)* **14**, 151–162.

Chatterjee, S. & Callaway, E.M. (2002). S cone contributions to the magnocellular visual pathway in macaque monkey. *Neuron* **35**, 1135–1146.

Chichilnisky, E.J. & Baylor, D.A. (1999). Receptive-field microstructure of blue-yellow ganglion cells in primate retina. *Nature Neuroscience* **2**, 889–893.

Croner, L.J. & Albright, T.D. (1997). Image segmentation enhances discrimination of motion in visual noise. *Vision Research* **37**, 1415–1427.

Cropper, S.J. & Derrington, A.M. (1994). Motion of chromatic stimuli: First-order or second-order? *Vision Research* **34**, 49–58.

Cropper, S.J. & Derrington, A.M. (1996). Rapid color-specific detection of motion in human vision. *Nature* **379**, 72–74.

Cropper, S.J., Mullen, K.T. & Badcock, D.R. (1996). Motion coherence across cardinal axes. *Vision Research* **36**, 2475–2488.

Cropper, S.J. & Wuerger, S.M. (2005). The perception of motion in chromatic stimuli. *Behavioral and Cognitive Neuroscience Reviews* **4**, 192–217.

Curcio, C.A., Allen, K.A., Sloan, K.R., Lerea, C.L., Hurley, J.B., Klock, I.B. & Milam, A.H. (1991). Distribution and morphology of human cone photoreceptors stained with anti-blue opsin. *Journal of Comparative Neurology* **312**, 610–624.

Dacey, D.M. & Lee, B.B. (1994). The 'blue-on' opponent pathway in primate retina originates from a distinct bistratified ganglion cell type. *Nature* **367**, 731–735.

Derrington, A.M. & Badcock, D.R. (1985). The low-level motion system has both chromatic and luminance inputs. *Vision Research* **25**, 1869–1878.

Derrington, A.M. & Henning, G.B. (1993). Detecting and discriminating the direction of motion of luminance and color gratings. *Vision Research* **33**, 799–811.

Derrington, A.M., Krauskopf, J. & Lennie, P. (1984). Chromatic mechanisms in lateral geniculate nucleus of macaque. *Journal of Physiology* **357**, 241–265.

DeValois, R.L., Cottaris, N.P., Elfar, S.D., Mahon, L.E. & Wilson, J.A. (2000). Some transformations of color information from lateral geniculate nucleus to striate cortex. *Proc. Natl. Ac. Sci. US* **97**, 4997–5002. **?1?**

Dougherty, R.F., Press, W.A. & Wandell, B.A. (1999). Perceived speed of colored stimuli. *Neuron* **24**, 893–899.

Edwards, M. & Badcock, D.R. (1996). Global-motion perception: Interaction of chromatic and luminance signals. *Vision Research* **36**, 2423–2431.

Hendry, S.H. & Reid, R.C. (2000). The Koniocellular Pathway in Primate Vision. *Annual Review of Neuroscience* **23**, 127–153.

Kooi, F.L. & DeValois, K.K. (1992). The role of color in the motion system. *Vision Research* **32**, 657–668.

Krauskopf, J. & Farell, B. (1990). Influence of color on the perception of coherent motion. *Nature* **348**(22 November), 328–331.

Levinson, E.S.R. (1975). The independence of channels in human vision selective for direction of motion. *Journal of Physiology (London)* **250**, 347–366.

Li, H.-C., O. & Kingdom, F.A.A. (2001). Segregation by color/luminance does not necessarily facilitate motion discrimination in the presence of motion distractors. *Perception & Psychophysics* **63**, 660–675.

Lindsey, D.T. & Teller, D.Y. (1990). Motion at isoluminance: discrimination/detection ratios for moving isoluminant gratings. *Vision Research* **30**, 1751–1761.

Metha, A.B. & Mullen, K.T. (1998). Failure of direction discrimination at detection threshold for both fast and slow chromatic motion. *Journal of the Optical Society of America A* **15**, 2945–2950.

Metha, A.B., Vingrys, A.J. & Badcock, D.R. (1994). Detection and discrimination of moving stimuli: the effects of color, luminance and eccentricity. *Journal of the Optical Society of America A* **11**, 1697–1709.

Møller, P. & Hurlbert, A. (1997). Interactions between color and motion in image segmentation. *Current Biology* **7**, 105–111.

Møller, P. & Hurlbert, A.C. (1997). Motion edges and regions guide image segmentation by color. *Proceedings of the Royal Society London Series B* **264**, 1571–1577.

Morand, S., Thut, G., Grave de Peralta, R., Clarke, S., Khateb, A., Landis, T. & Michel, C.M. (2000). Electrophysiological evidence for fast visual processing through the human koniocellular pathway when stimuli move. *Cerebral Cortex* **10**, 817–825.

Mullen, K.T. (1985). The contrast sensitivity of human color vision to red-green and yellow-blue chromatic gratings. *Journal of Physiology* **359**, 381–400.

Mullen, K.T. (1991). Color vision as a post-receptoral specialization of the central visual field. *Vision Research* **31**, 119–130.

Mullen, K.T. & Baker, C.L. (1985). A motion after-effect from an isoluminant stimulus. *Vision Research* **25**, 685–688.

Mullen, K.T. & Boulton, J.C. (1992). Interactions between color and luminance contrast in the perception of motion. *Ophthalmic and Physiological Optics* **12**, 201–205.

Mullen, K.T. & Kingdom, F.A.A. (2002). Differential distributions of red-green and blue-yellow cone opponency across the visual field. *Visual Neuroscience* **19**, 109–118.

Newsome, W.T. & Pare, E.B. (1988). A selective impairment of motion perception following lesions of the middle temporal visual area (MT). *Journal of Neuroscience* **8**, 2201–2211.

Palmer, J., Mobley, L.A. & Teller, D.Y. (1993). Motion at isoluminance: discrimination/detection ratios and the summation of luminance and chromatic signals. *Journal of the Optical Society of America, A* **10**, 1353–1362.

Ramachandran, V.S. (1987). Interaction between color and motion in human vision. *Nature* **328**, 645–647.

Ramachandran, V.S. & Gregory, R.L. (1978). Does color provide an input to human motion perception? *Nature* **275**, 55–56.

Regan, B.C., Reffin, J.P. & Mollon, J.D. (1994). Luminance noise and the rapid determination of discrimination ellipses in color deficiency. *Vision Research* **34**, 1279–1299.

Ruppertsberg, A.I., Wuerger, S.M. & Bertamini, M. (2003). The chromatic selectivity of global motion processing. *Visual Neuroscience* **20**, 421–428.

Seidemann, E., Poirson, A.B., Wandell, B.A. & Newsome, W.T. (1999). Color signals in area MT of the macaque monkey. *Neuron* **24**, 911–917.

Sincich, L.C. & Horton, J.C. (2005). The circuitry of V1 and V2: Integration of color, form and motion. *Annual Review of Neuroscience* **28**, 303–326.

Sincich, L.C., Park, K.F., Wohlgemuth, M.J. & Horton, J.C. (2004). Bypassing V1: a direct geniculate input to area MT. *Nature Neuroscience* **7**, 1123.

Snowden, R. J. & Edmunds, R. (1999). Color and polarity contributions to global motion perception. *Vision Research* **39**, 1813–1822.

Stromeyer III, C.F., Chaparro, A., Rodriguez, C., Chen, D., Hu, E. & Kronauer, R.E. (1998). Short-wave cone signal in the red-green detection mechanism. *Vision Research* **38**, 813–826.

Stromeyer III, C.F., Kronauer, R.E., Ryu, A., Chaparro, A. & Eskew Jr., R.T. (1995). Contribution of human long-wave and middle-wave cones to motion. *Journal of Physiology* **485**, 221–243.

Walsh, J.W.T. (1958). *Photometry*, 3rd ed. London: Constable & Co. Ltd.

Wandell, B. (1993). *Foundations of Vision*. Sunderland, MA: Sinauer Associates, Inc.

Wandell, B.A., Poirson, A.B., Newsome, W.T., Baseler, H.A., Boynton, G.M., Huk, A., Gandhi, S. & Sharpe, L.T. (1999). Color signals in human motion-selective cortex. *Neuron* **24**, 900–909.

Watson, A.B. & Pelli, D. (1983). QUEST: A Bayesian adaptive psychometric method. *Perception & Psychophysics* **33**, 113–120.

Watson, A.B., Thompson, P.G., Murphy, B.J. & Nachmias, J. (1980). Summation and discrimination of gratings moving in opposite directions. *Vision Research* **20**, 341–347.